Expansion of epigenetic alterations in *EFEMP1* promoter predicts malignant formation in pancreatobiliary intraductal papillary mucinous neoplasms

Running Title: Epigenetic alterations in EFEMP1 in IPMN

Authors: Kazuhiro Yoshida MD,[1] Takeshi Nagasaka MD, PhD,[1§] Yuzo Umeda MD, PhD,[1] Takehiro Tanaka, MD, PhD,[2] Keisuke Kimura MD,[1] Fumitaka Taniguchi MD,[1] Tomokazu Fuji MD,[1] Kunitoshi Shigeyasu MD, PhD,[1] Yoshiko Mori MD,[1] Hiroyuki Yanai MD, PhD,[2] Takahito Yagi MD, PhD,[1] Ajay Goel PhD,[3] and Toshiyoshi Fujiwara MD, PhD,[1]

[1]Department of Gastroenterological Surgery, [2]Pathology, Okayama University Graduate School of Medicine, Dentistry and Pharmaceutical Sciences, Okayama City, Okayama 700-8558, Japan;

[3]Center for Gastrointestinal Cancer Research; Center for Epigenetics, Cancer Prevention and Cancer Genomics, Baylor Research Institute and Charles A Sammons Cancer Center, Baylor University Medical Center, Dallas, TX 75246, USA.

[§]***Corresponding author:*** Takeshi Nagasaka, MD., Ph.D., Department of Gastroenterological Surgery, Okayama University Graduate School of Medicine, Dentistry and Pharmaceutical Sciences, 2-5-1

Shikata-cho, Kita-ku, Okayama City, Okayama 700-8558, Japan,

Tel.: +81-86-235-7257; Fax: +81-86-223-8775

E-mail address: takeshin@cc.okayama-u.ac.jp

Authors' contributions: KY extracted DNA, performed methylation and genetic analyses, and drafted the manuscript. TN assisted with data interpretation, designed the project, secured the funding, and drafted the manuscript. YU and TY provided patient samples and clinicopathological data. TT and HY performed IHC and pathological investigations. KK and FT assisted with *KRAS* and *GNAS* mutation analysis and provided clinical information. TomF, YM, and SK assisted with IHC staining and summarized clinicopathological data. AG assisted with data interpretation and revised the manuscript. TosF provided patient samples and clinicopathological data, assisted with data interpretation, and revised the manuscript. All authors have read and approved the final manuscript.

Abstract

Purpose: Although limited understanding exists for the presence of specific genetic mutations and aberrantly methylated genes in pancreatobiliary intraductal papillary mucinous neoplasms (IPMNs), the fundamental understanding of the dynamics of methylation expansion across CpG dinucleotides in specific gene promoters during carcinogenesis remains unexplored. Expansion of DNA methylation in some gene promoter regions, such as *EFEMP1*, one of the fiblin family, with tumor progression has been reported in several malignancies. We hypothesized that DNA hypermethylation in *EFEMP1* promoter would expand with the tumor grade of IPMN.

Methods: A sample of 65 IPMNs and 30 normal pancreatic tissues was analyzed. IPMNs were divided into the following three subsets according to pathological findings: 31 with low-grade dysplasia (low grade), 11 with high-grade dysplasia (high grade), and 23 with associated invasive carcinoma (invasive Ca). Mutations in the *KRAS* or *GNAS* genes were analyzed by Sanger sequencing, and methylation status of two discrete regions within the *EFEMP1* promoter, namely region 1 and region 2, were analyzed by bisulfite sequencing and fluorescent high-sensitive assay for bisulfite DNA (Hi-SA). Expression status of EFEMP1 was investigated by immunohistochemistry (IHC).

Results: *KRAS* mutations were detected in 39%, 55%, and 70% of low grade, high grade, and invasive Ca, respectively. *GNAS* mutations were observed in 32%, 55%, and 22% of low grade, high grade, and invasive Ca, respectively. The methylation of individual regions (region 1 or 2) in the *EFEMP1* promoter

was observed in 84%, 91%, and 87% of low grade, high grade, and invasive Ca, respectively. However, simultaneous methylation of both regions (extensive methylation) was exclusively detected in 35% of invasive Ca (P = 0.001) and five of eight IPMNs (63%) with extensive methylation, whereas 20 of 57 (35.1%) tumors of unmethylation or partial methylation of the *EFEMP1* promoter region showed weak staining EFEMP1 in extracellular matrix (P = 0.422). In addition, extensive *EFEMP1* methylation was particularly present in malignant tumors without *GNAS* mutations and associated with disease-free survival of patients with IPMNs (P < 0.0001).

Conclusions: Extensive methylation of the *EFEMP1* gene promoter can discriminate invasive from benign IPMNs with superior accuracy owing to their stepwise accumulation of tumor progression.

Key words: mucinous neoplasms, methylation, epigenetics, EFEMP1, invasive carcinoma, dysplasia

Introduction

Pancreatic intraductal papillary mucinous neoplasms (IPMNs) are precursor lesions characterized by an atypical degree of intraductal proliferation of neoplastic mucinous cells arising in the pancreatic duct (Das et al. 2013; Matthaei et al. 2012; Tanaka et al. 2012; Wasif et al. 2010). Histologically, IPMNs may progress from low-grade to high-grade dysplasia and finally to an invasive carcinoma (Das et al. 2013; Farrell and Brugge 2002; Salvia et al. 2004), canonical to the adenoma-carcinoma sequence in colorectal cancer and pancreatic ductal adenocarcinoma (PDAC) (Wasif et al. 2010). While IPMNs with invasive carcinoma have a poor 5-year survival ratio of 33%–43%, patients with resected IPMNs without any invasive cancer features generally have a better 5-year survival ratio of 77%–94% (Chari et al. 2002; Das et al. 2013; Farrell and Brugge 2002; Maire et al. 2002; Raimondo et al. 2002; Sohn et al. 2004), highlighting the importance of efficient diagnosis of IPMNs with invasive carcinoma. Therefore, preoperative identification of dysplastic IPMNs is challenging even with a multimodality approach including radiographic imaging, endoscopic ultrasound-guided fine-needle aspiration (EUSFNA), cytological examination, and tumor markers (Schoedel et al. 2006). This problem has prompted the development of other analytical tools, including genomic biomarkers that can predict IPMNs at a high risk of developing dysplasia with malignant potential (Schoedel et al. 2006).

Applying molecular techniques to evaluate surgical and cytological specimens is evolving in conjunction with our understanding of the IPMN molecular makeup (Schoedel et al. 2006). Studies aimed

at characterizing genetic profiles in IPMNs have identified activating mutations of *KRAS* and *GNAS* oncogenes and inactivating mutations in *RNF43*, *CDKN2A/p16*, and *TP53* tumor suppressor genes (Amato et al. 2014; Cooper et al. 2013; Dal Molin et al. 2013; Furukawa et al. 2011; Kanda et al. 2013; Komatsu et al. 2014; Schonleben et al. 2007; Schonleben et al. 2008; Sessa et al. 1994). Collectively, these studies underscored the importance of genetic alterations in IPMN progression; however, the prevalence of such genetic events generally occurs at lower frequencies than in PDAC (Adsay 2002; Cooper et al. 2013; Kanda et al. 2013; Sato and Goggins 2006).

Similar to other cancers, epigenetic alterations, such as promoter hypermethylation of tumor suppressor genes, are considered a critical process in IPMN development (Sato and Goggins 2006). Results suggest a gradual expansion of methylation across CpG islands in *MGMT*, *RASSF2*, and *SFRP2* promoters during colorectal cancer progression and highlighted their potential role as biomarkers for diagnosis and disease prediction for specific cancer types (Nagasaka et al. 2008; Nagasaka et al. 2009; Takeda et al. 2011). In this study, we evaluated the methylation status of the epidermal growth factor-containing fibulin-like extracellular matrix protein 1 gene (*EFEMP1*, alternative annotation is *FIbulin3*), a member of the fibulin family of extracellular matrix (ECM) proteins. EFEMP1 is involved in malignant transformation through modulation of cell proliferation, angiogenesis, and invasion in a tissue-dependent manner (Kobayashi et al. 2007; Sadr-Nabavi et al. 2009; Wang et al. 2010; Wang et al. 2012; Yang et al. 2013; Yue et al. 2007; Zhu et al. 2014), and alterations in this gene expression have

often been linked to aberrant DNA methylation (Nomoto et al. 2010; Sadr-Nabavi et al. 2009; Wang et al. 2010; Wang et al. 2012; Yang et al. 2013; Yue et al. 2007; Zhu et al. 2014). Moreover, recent studies have reported an association between a reduction in protein expression and*EFEMP1* methylation expansion in breast and lung cancers using immunohistochemistry and sequencing approaches (Chen et al. 2014; Sadr-Nabavi et al. 2009). For these reasons, the presence or absence of methylation and gradual expansion of specific gene promoter methylation may help diagnose and differentiate invasive carcinoma from normal adjacent tissues and dysplastic lesions.

To systematically test this hypothesis, we first analyzed mutations in the *KRAS* and *GNAS* genes to confirm the genetic background of IPMNs. Next, to determine whether extensive methylation of candidate genes may serve as a predictive alteration for malignant IPMNs, we performed a comprehensive investigation of the methylation status of *EFEMP1* promoter and examined EFEMP1 expression status by IHC.

Materials and Methods

Samples and Tumor Classifications

Nine tissues from non-necrotic areas of PDAC were frozen immediately at −80°C, and DNA was extracted from the tissues using QIAamp DNA mini kits (Qiagen, Valencia, CA, USA). DNAs of 21 tissues from non-necrotic areas of PDAC were macrodissected from formalin-fixed, paraffin-embedded (FFPE) specimens. DNAs of IPMNs were macrodissected from 65 patients who underwent surgical resection and who were pathologically diagnosed with IPMNs or invasive IPMNs. All samples were collected from the Okayama University Hospital, Okayama, Japan, between January 2001 and December 2012. Institutional review board approval was granted by the ethics committee of the Okayama University, and written informed consent was obtained from all patients to use their tissues for research. The medical records of the patients were retrospectively explored and matched with clinical and pathological data. We defined IPMN classification based on the International Consensus Guidelines from 2012 as follows: MD-IPMNs were characterized by segmental or diffused dilation of the main pancreatic duct by >5 mm in the absence of other causes of obstruction; BD-IPMNs comprised pancreatic cysts of >5 mm in diameter communicating with the main pancreatic duct; finally, mixed-type lesions were those lesions that simultaneously met the criteria of both MD-IPMNs and BD-IPMNs (Tanaka et al. 2012). In addition, we used a revised terminology to classify IPMNs. Formally, IPMNs are classified according to World Health Organization classification based on pathological findings as follows: IPMNs with low-grade

dysplasia, intermediate-grade dysplasia, high-grade dysplasia (carcinoma in situ) and with an associated invasive carcinoma. Based on the revised classification criteria proposed in 2015, IPMNs with intermediate-grade dysplasia are combined together with the ones with low-grade dysplasia and are now called low-grade IMPNs. Therefore, we classified IPMNs according to this revised nomenclature.

IPMN patients' characteristics

Using the criteria mentioned above, our sample of 65 IPMNs was classified as follows: 31 (48%), 11 (17%), and 23 (35%) IPMNs were classified as low- or intermediate-grade dysplasia (low grade), high-grade dysplasia (high grade), and invasive Ca, respectively. To clarify the clinicopathological features of IPMNs, statistical analyses were performed between low grade and high grade and invasive Ca (Supplementary Table 1). Within the group of 23 invasive Ca, only one case showed a distant metastasis in the liver at surgical resection (and hence classified as stage IV); the remainder of the invasive Ca cases was categorized as stage I (10 of 23; 44%) and stage II (12 of 23; 52%, Supplementary Table 2). Disease free survival (DFS) and overall survival (OS) of IPMNs were estimated according to their clinicopathological characteristics (Supplementary Fig. 1). The median time of the follow-up period of 65 IPMNs after surgical resection was 48 months (range, 8–108 months). The lesions categorized as invasive Ca were also classified by the tumor node metastasis classification system (Adsay et al. 2010; Kim et al. 2008).

Direct sequencing of KRAS and GNAS mutations in IPMNS tissues

KRAS mutations in codons 12 and 13 were determined by the method previously described (Nagasaka et al. 2008; Nagasaka et al. 2009; Takeda et al. 2011). *GNAS* mutations in codon 201 were analyzed by direct sequencing using *GNAS* primers (Supplementary Fig. 2 and Supplementary Table 3).

Analysis of DNA methylation

DNA was subjected to sodium bisulfite modification using the EZ DNA Methylation Kit (ZYMO Research, Irvine, CA). As shown in Figure 1, methylation status of the *EFEMP1* gene promoter was studied at various regions in previous studies (Kobayashi et al. 2007; Nomoto et al. 2010; Sadr-Nabavi et al. 2009; Wang et al. 2010; Wang et al. 2012; Yang et al. 2013; Yue et al. 2007; Zhu et al. 2014). In this study, we searched CTCF biding sites by CTCFBSDB 2.0 (http://insulatordb.uthsc.edu/) in promoter region of the *EFEMP1* gene and found a CTCF biding site 'TGACATCTGTTGGG', called as the EMBL_M1 motifs (Schmidt et al. 2012). CTCF, also known as CCCTC-binding factor, is a transcription factor involved in many cellular processes, including transcriptional regulation, insulator activity, V(D)J recombination and regulation of chromatin architecture (Chaumeil and Skok 2012; Phillips and Corces 2009). Interestingly, this biding site was between the two regions which were analyzed by previous studies as mentioned above. For the reason, we divided the *EFEMP1* gene promoter into two regions

(regions 1 and 2, Fig. 1), which were located as dividing line on the CTCF biding site, and analyzed by a fluorescence high-sensitive assay (Hi-SA) using bisulfite-modified DNA template as previously described (Nagasaka et al. 2009). The sense and antisense nonspecific primers and internal methylation-specific primers with enhanced sensitivity for polymerase chain reaction (PCR) amplification have been described previously (Nagasaka et al. 2009) and are shown in Supplementary Table 3. PCR products digested with *HhaI* (New England BioLabs, Massachusetts, USA) were loaded simultaneously onto an ABI 310R or 31000 Genetic Analyzer (Applied Biosystems, California, USA). Signals from individual PCR products were distinguished by the unique fluorescent PCR signal from each target and their fragment length, and the data were analyzed using GeneMapper software version 4.0 (Applied Biosystems, California, USA). In this study, the percentages of methylated *HhaI* sites were calculated by determining the ratios between the *HhaI*-cleaved PCR product and the total amount of PCR product in each loci, and methylation positivity was defined as a proportion of >1.0% of methylated *HhaI* sites. Direct sequencing of the two regions in the *EFEMP1* promoter was performed by PCR products obtained from bisulfite DNA extracted from normal pancreatic tissues and IPMNs. Primer sequences are shown in Supplementary Table 3.

Immunohistochemical Analysis

EFEMP1 localization was performed by immunohistochemical (IHC). A sample of 65 IPMNs was available for IHC staining for EFEMP1 protein expression analysis. Staining was carried out manually

with FFPE tissues. Thin (5 μm) sections of representative blocks were deparaffinized and dehydrated using gradient solvents. Following antigen retrieval in the citrate buffer (pH 6.0), endogenous peroxidase was blocked with 3% H_2O_2. Thereafter, slides were incubated overnight in the presence of a purified mouse anti-human EFEMP1 monoclonal antibody (sc-33722, Santa Cruz, Dallas, TX, USA; dilution 1:250). Further incubation was carried out with a secondary antibody and the avidin–biotin–peroxidase complex (Vector Laboratories, Burlingame, CA, USA) and then incubated with biotinyl-tyramide followed by streptavidin-peroxidase. Diaminobenzidine was used as a chromogen and hematoxylin as a nuclear counterstain.

EFEMP1 was detectable in normal pancreatic tissue; weak staining was detected in islets of Langerhans, whereas intense staining was observed in the peripheral nerve fiber. IHC results were interpreted by pathologists blinded to the corresponding clinicopathological data. The expression status of EFEMP1 was evaluated by an immunoreactive score (IRS), which was calculated by scoring of the percentage of positive cells and their expression intensities. The percentage of positive ECM staining was rated as described previously and as follows: 1 = 0%–10%, 2 = 11%–50%, 3 = 51%–80%, and 4 = 81%–100% (Sadr-Nabavi et al. 2009). Staining intensity was scored as follows: 1 = weak, 2 = moderate, and 3 = intensive. All IPMNs were categorized into four subsets by IRS score as follows: 0-1 = no staining, 2-3 = weak staining, 4–8 = moderate staining, and 9–12 = strong staining (Remmele and Stegner 1987).

Statistical Analyses

All statistical analyses were performed using EZR (Saitama Medical Center, Jichi Medical University), which is a graphical user interface for R (The R Foundation for Statistical Computing, version 2.13.0). First, methylation levels were analyzed as continuous variables. Next, the methylation status was analyzed as a categorical variable (positive, methylation level > 1.0%; negative, methylation level $\leq$ 1.0%), as described previously. Each IPMN specimen was given a numerical score so as to reflect the number of methylated loci. Categorical variables were compared by Fisher's exact test. Differences between continuous variables were determined using the Mann–Whitney *U* test or the Kruskal–Wallis test. Multiple comparisons were performed using the Steel–Dwass test. OS was calculated from the date of surgical resection to the date of death due to IPMNS or last follow-up for censored patients. DFS was calculated from the date of surgical resection to the date of the first documentation of local, regional, or distant relapse, appearance of a second primary lesion by computed tomography and/or magnetic resonance imaging routinely performed per 6 months. OS and DFS were univariately estimate with the Kaplan–Meier method. All *P*-values reported were calculated by two-sided tests, and values <0.05 were considered statistically significant.

Results

KRAS *and* GNAS *mutations in IPMNs*

To evaluate the genetic background in our current cohort, we analyzed mutations in *KRAS* and *GNAS* genes as shown in Supplementary Figure 2. *KRAS* mutations were detected in 33 IPMNs (51%), and the spectrum of relative frequencies of individual mutations was 5 (15% of *KRAS* mutants), 12 (36%), and 16 (49%) for G12R, G12D, and G12V mutations, respectively (Supplementary Tables 1 and 2). Meanwhile, 19 IPMNs (29%) harbored *GNAS* mutations, and the following mutations were primarily found in codon 201: R201H, 5 IPMNs (26%); R201C, 13 IPMNs (68%); and R201S, 1 IPMNs (5%) (Table 2). One R201S was a novel mutation, which had not been previously described for IPMNs. *KRAS* mutation frequency tended to increase with IPMN grade: 12 of 31 were low grade (39%), 6 of 11 were high grade (55%), and 16 of 23 were invasive Ca (70%, $P = 0.084$; low grade vs. high grade/invasive Ca). In contrast, *GNAS* mutations were constantly observed, with 10 of 32 (32%) in low grade and 12 of 33 (36%) in high grade and invasive Ca. Concurrent *KRAS* and *GNAS* mutations were observed in 11 IPMNs (17%), *KRAS* mutation were present only in 22 IPMNs (34%), *GNAS* mutations only in 8 IPMNs (12%), and wild-type status of both genes was observed in 24 IPMNs (37%, Supplementary Fig. 2C).

We assessed DFS and OS according to *KRAS* or *GNAS* mutation status. Although *KRAS* mutations were more frequently observed in invasive Ca, there was no difference in outcome between *KRAS* mutants and wild type (Supplementary Fig. 2E and F). In contrast, *GNAS* mutations were less frequently

observed in invasive Ca compared with low and high grade, and there was no difference in outcome between *GNAS* mutants and wild type (Supplementary Fig. 2G and H).

Methylation profiles of* EFEMP1 *promoter in IPMNs

We investigated the methylation status of discrete regions in the *EFEMP1* promoter in 65 IPMNs and 30 normal pancreatic tissues obtained from PDAC patients. The location of the *EFEMP1* gene and a panel of representative bisulfite sequencing and fluorescent Hi-SA results are depicted in Fig. 1 and Fig. 2A, respectively. Methylation status in the discrete regions obtained from fluorescent Hi-SA was analyzed as the categorical variable. Figure 2B presents methylation frequency in each discrete region according to pathological features, and Table 1 presents the correlation between the methylation status of *EFEMP1* and the clinical and pathological features of IPMNs. The region-1 methylation was frequently observed in invasive Ca ($P = 0.0016$), whereas the region-2 methylation was commonly observed in IPMN (>80% of IPMNs) but less frequently in normal pancreatic tissues (<20%). Another interesting feature of IPMNs with extensive *EFEMP1* methylation was histologic subtype, in which extensive *EFEMP*1 methylation was frequently observed in pancreatobiliary type lesions (4 of 6; 67%, $P = 0.027$).

With respect to *KRAS/GNAS* mutation status, interestingly, IPMNs with methylation of the region-1 never harbored *GNAS* mutations (0 of 10; 0%, $P = 0.028$), while 7 of 10 IPMNs with methylation of the region-1 harbored *KRAS* mutations (70%). While methylation of the region-2 promoter

was frequently observed (54 of 65 IPMNs [83%]), no associations were observed among the frequencies of region-2 methylation and any of the clinicopathological factors.

Next, we evaluated correlations between the methylation status of *EFEMP1* promoter and the clinicopathological features of invasive Ca (Supplementary Table 3). However, methylation status had no association with any of the features explored in invasive Ca.

Finally, we also assessed DFS and OS according to methylation status in the discrete *EFEMP1* promoter regions. As extensive *EFEMP1* methylation was a specific feature of invasive Ca, IMPNs with extensive *EFEMP1* methylation showed a poor prognosis compared with IMPNs without extensive *EFEMP1* methylation (Fig. 2C and D).

Association of* EFEMP1 *promoter methylation and protein expression

We investigated EFEMP1 protein expression in 65 IPMN tissues. Representative examples of IHC staining results are shown in Figure 3A–C. Using these criteria, no IPMNs were categorized as having no staining, whereas 25, 38, and 2 IPMNs were deemed to have weak, moderate, and strong staining, respectively. Although five of eight IPMNs (63%) showed weak staining and extensive methylation of the *EFEMP1* promoter region, no significant differences in the frequencies of EFEMP1 protein expression were observed in IPMNs exhibiting partial methylation or non-methylation in the *EFEMP1* promoter (Fig. 3D).

Discussion

We have shown for the first time the biological significance of methylation in discrete promoter regions of *EFEMP1* gene in tissue specimens obtained from patients with pancreatobiliary IPMNs, playing an important functional role in malignant transformation by modulating cell proliferation, angiogenesis, and invasion in a tissue-dependent context (Kobayashi et al. 2007); it is a common target of promoter hypermethylation in various tumors (Nomoto et al. 2010; Sadr-Nabavi et al. 2009; Wang et al. 2010; Wang et al. 2012; Yang et al. 2013; Yue et al. 2007; Zhu et al. 2014). Aberrant hypermethylation of the *EFEMP1* promoter region is a potential biomarker. Sadr et al. reported an association between reduction in protein expression and *EFEMP1* methylation expansion in breast cancer using sequencing approaches and IHC (Sadr-Nabavi et al. 2009). In this study, we also examined the association between EFEMP1 expression in ECM by IHC and *EFEMP1* methylation profiles. Unfortunately, although 63% of IPMNs with extensive methylation of the *EFEMP1* promoter region showed weak staining in ECM, no significant differences in the frequencies of EFEMP1 protein expression were observed in IPMNs exhibiting partial methylation or non-methylation in the *EFEMP1* promoter.

Considering the importance of *EFEMP1*, we hypothesized that gradual expansion of methylation across its promoter during the development of IPMN serves as a biomarker for distinguishing malignant IPMNs from the non-malignant ones. To systematically test this hypothesis, we first analyzed mutations in the *KRAS* and *GNAS* oncogenes to confirm the genetic background of IPMNs. Usually, the methylation

pattern in a gene promoter is considered either entirely methylated or non-methylated. However, as demonstrated by bisulfite sequencing, individual CpG residues within the *EFEMP1* promoter were not equally methylated. In this study, region-2 of the *EFEMP1* promoter was more frequently methylated than region-1, and the aberrant methylation tended to spread from region-2 toward region-1 with IPMN progression. More importantly, none of the normal pancreatic tissues, low or high grade IMPNs showed extensive methylation in the *EFEMP1* promoter. These characteristics of the *EFEMP1* methylation pattern in IPMN carcinogenesis appeared similar to those of *MGMT*, *SFRP2*, and *RASSF2* in the adenoma-carcinoma sequence of colorectal cancer (Nagasaka et al. 2008; Nagasaka et al. 2009; Takeda et al. 2011). Therefore, the presence or absence of methylation and the gradual expansion of methylation of specific gene promoters may help diagnose and differentiate invasive carcinoma from normal adjacent tissues and dysplastic lesions. This fundamental concept of stepwise expansion of DNA methylation across specific gene promoters during the neoplastic progression of IPMNs remains unexplored and is still an active area of investigation.

KRAS and *GNAS* mutations, the most common genetic mutations observed in IPMNs, occurred in the early stages of disease progression. *KRAS* and *GNAS* mutations were also found at codon 12 (a G12D, G12V, or G12R) and codon 201 (an R201H or R201C), respectively. These genetic features are in line with those previously reported in other studies (Amato et al. 2014; Furukawa et al. 2011; Sadr-Nabavi et al. 2009; Wu et al. 2011a; Wu et al. 2011b). This agreement indicates that *KRAS* mutations at codon 12 or

GNAS mutations at codon 201 could play a key role as the driver of carcinogenesis, providing a selective advantage in tumor formation associated with these IPMNs (Parmigiani et al. 2009). However, the frequencies of both genetic mutations, especially *GNAS* mutations, were different among genetic mutational analyses. In the current study, *GNAS* mutations were observed with similar frequencies in low grade and invasive Ca. However, Furukawa et al. reported that *GNAS* mutations were more common in low-grade lesions (Furukawa et al. 2011). In contrast, Amato et al and other authors showed that *GNAS* mutation frequency tended to increase with tumor progression (Amato et al. 2014; Wu et al. 2011a; Wu et al. 2011b). These differences in observations might partly be due to smaller sample size or variations in the detection technologies used in the studies.

To our knowledge, no studies have been published so far demonstrating a correlation between genetic and epigenetic alterations in IPMNs although several previous reports have revealed that there are distinct patterns of genetic mutations in IPMN subtypes (Amato et al. 2014; Chadwick et al. 2009; Cooper et al. 2013; Dal Molin et al. 2013; Fritz et al. 2009; Komatsu et al. 2014; Mino-Kenudson et al. 2011; Mohri et al. 2012). In this study, extensive methylation of *EFEMP1* was likely to occur in IPMNs without *GNAS* mutations (Table 2). This result might reflect the biological behavior of the *GNAS* gene pathway, which is less aggressive than that of the *KRAS* gene, and further investigation is needed to evaluate the roles of *KRAS* and *GNAS* mutations in IPMN carcinogenesis.

Our study has several limitations. One is the sample size. Another is that, although we examined

the correlation between methylation status of our analyzed regions in the *EFEMP* promoter and its expression status by IHC, there was no strong correlation between them; hence, further investigation is needed. Beyond the limitations, we demonstrated that the extensive methylation in the *EFEMP1* promoter could be a useful predictive marker for invasive IPMNs and could serve as a possible means to noninvasively screen for invasive IPMNs using DNA obtained from EUSFNA, pancreatic juice, and fecal samples.

Acknowledgments: The authors would like to thank Mr. Toru Nakai, Mrs. Tae Yamanishi, and Mr. Akihiro Nyuya for technical assistance and Enago (www.enago.jp) for English language editing.

Compliance with Ethical Standards

Funding:

This study was funded by KAKENHI (20590572, 25860409, 26462016, and 15H03034).

Conflict of Interest:

All the authors declare that they have no conflict of interest

Ethical approval:

All procedures were performed in accordance with the ethical standards of the institutional and/or national research committee and with the 1964 Helsinki declaration and its later amendments or comparable ethical standards.

Informed consent:

Informed consent was obtained from all individual participants included in the study.

References

Adsay NV (2002) Intraductal papillary mucinous neoplasms of the pancreas: pathology and molecular genetics J Gastrointest Surg 6:656-659

Adsay NV, Fukushima N, Furuawa T, et al. (2010) Intraductal neoplasm of the pancreas. In: Bosman FT, Carneiro F, Hruban RH, Theise ND (eds) WHO classification of tumors of digestive system. Lyon, pp 304-313

Amato E et al. (2014) Targeted next-generation sequencing of cancer genes dissects the molecular profiles of intraductal papillary neoplasms of the pancreas J Pathol 233:217-227 doi:10.1002/path.4344

Chadwick B, Willmore-Payne C, Tripp S, Layfield LJ, Hirschowitz S, Holden J (2009) Histologic, immunohistochemical, and molecular classification of 52 IPMNs of the pancreas Appl Immunohistochem Mol Morphol 17:31-39 doi:10.1097/PAI.0b013e31817c02c6

Chari ST et al. (2002) Study of recurrence after surgical resection of intraductal papillary mucinous neoplasm of the pancreas Gastroenterology 123:1500-1507

Chaumeil J, Skok JA (2012) The role of CTCF in regulating V(D)J recombination Curr Opin Immunol 24:153-159 doi:10.1016/j.coi.2012.01.003

Chen X, Meng J, Yue W, Yu J, Yang J, Yao Z, Zhang L (2014) Fibulin-3 suppresses Wnt/beta-catenin signaling and lung cancer invasion Carcinogenesis 35:1707-1716 doi:10.1093/carcin/bgu023

Cooper CL, O'Toole SA, Kench JG (2013) Classification, morphology and molecular pathology of

premalignant lesions of the pancreas Pathology 45:286-304 doi:10.1097/PAT.0b013e32835f2205

Dal Molin M et al. (2013) Clinicopathological correlates of activating GNAS mutations in intraductal papillary mucinous neoplasm (IPMN) of the pancreas Ann Surg Oncol 20:3802-3808 doi:10.1245/s10434-013-3096-1

Das KK et al. (2013) mAb Das-1 is specific for high-risk and malignant intraductal papillary mucinous neoplasm (IPMN) Gut 63:1626-1634 doi:10.1136/gutjnl-2013-306219

Farrell JJ, Brugge WR (2002) Intraductal papillary mucinous tumor of the pancreas Gastrointest Endosc 55:701-714

Fritz S et al. (2009) Global genomic analysis of intraductal papillary mucinous neoplasms of the pancreas reveals significant molecular differences compared to ductal adenocarcinoma Ann Surg 249:440-447 doi:10.1097/SLA.0b013e31819a6e16

Furukawa T et al. (2011) Whole-exome sequencing uncovers frequent GNAS mutations in intraductal papillary mucinous neoplasms of the pancreas Sci Rep 1:161 doi:10.1038/srep00161

Kanda M et al. (2013) Mutant TP53 in duodenal samples of pancreatic juice from patients with pancreatic cancer or high-grade dysplasia Clin Gastroenterol Hepatol 11:719-730. e5 doi:10.1016/j.cgh.2012.11.016

Kim SC et al. (2008) Intraductal papillary mucinous neoplasm of the pancreas: clinical characteristics and treatment outcomes of 118 consecutive patients from a single center J Hepatobiliary Pancreat

Surg 15:183-188 doi:10.1007/s00534-007-1231-8

Kobayashi N et al. (2007) A comparative analysis of the fibulin protein family. Biochemical characterization, binding interactions, and tissue localization The Journal of biological chemistry 282:11805-11816 doi:10.1074/jbc.M611029200

Komatsu H et al. (2014) A GNAS mutation found in pancreatic intraductal papillary mucinous neoplasms induces drastic alterations of gene expression profiles with upregulation of mucin genes PLoS One 9:e87875 doi:10.1371/journal.pone.0087875

Maire F et al. (2002) Prognosis of malignant intraductal papillary mucinous tumours of the pancreas after surgical resection. Comparison with pancreatic ductal adenocarcinoma Gut 51:717-722

Matthaei H et al. (2012) Clinicopathological characteristics and molecular analyses of multifocal intraductal papillary mucinous neoplasms of the pancreas Ann Surg 255:326-333 doi:10.1097/SLA.0b013e3182378a18

Mino-Kenudson M et al. (2011) Prognosis of invasive intraductal papillary mucinous neoplasm depends on histological and precursor epithelial subtypes Gut 60:1712-1720 doi:10.1136/gut.2010.232272

Mohri D et al. (2012) Different subtypes of intraductal papillary mucinous neoplasm in the pancreas have distinct pathways to pancreatic cancer progression J Gastroenterol 47:203-213 doi:10.1007/s00535-011-0482-y

Nagasaka T et al. (2008) Methylation pattern of the O6-methylguanine-DNA methyltransferase gene in colon during progressive colorectal tumorigenesis Int J Cancer 122:2429-2436 doi:10.1002/ijc.23398

Nagasaka T et al. (2009) Analysis of fecal DNA methylation to detect gastrointestinal neoplasia J Natl Cancer Inst 101:1244-1258 doi:10.1093/jnci/djp265

Nomoto S et al. (2010) Epidermal growth factor-containing fibulin-like extracellular matrix protein 1, EFEMP1, a novel tumor-suppressor gene detected in hepatocellular carcinoma using double combination array analysis Ann Surg Oncol 17:923-932 doi:10.1245/s10434-009-0790-0

Parmigiani G, Boca S, Lin J, Kinzler KW, Velculescu V, Vogelstein B (2009) Design and analysis issues in genome-wide somatic mutation studies of cancer Genomics 93:17-21 doi:10.1016/j.ygeno.2008.07.005

Phillips JE, Corces VG (2009) CTCF: master weaver of the genome Cell 137:1194-1211 doi:10.1016/j.cell.2009.06.001

Raimondo M, Tachibana I, Urrutia R, Burgart LJ, DiMagno EP (2002) Invasive cancer and survival of intraductal papillary mucinous tumors of the pancreas Am J Gastroenterol 97:2553-2558 doi:10.1111/j.1572-0241.2002.06022.x

Remmele W, Stegner HE (1987) [Recommendation for uniform definition of an immunoreactive score (IRS) for immunohistochemical estrogen receptor detection (ER-ICA) in breast cancer tissue]

Pathologe 8:138-140

Sadr-Nabavi A et al. (2009) Decreased expression of angiogenesis antagonist EFEMP1 in sporadic breast cancer is caused by aberrant promoter methylation and points to an impact of EFEMP1 as molecular biomarker International journal of cancer 124:1727-1735 doi:10.1002/ijc.24108

Salvia R et al. (2004) Main-duct intraductal papillary mucinous neoplasms of the pancreas: clinical predictors of malignancy and long-term survival following resection Ann Surg 239:678-685; discussion 685-677

Sato N, Goggins M (2006) Epigenetic alterations in intraductal papillary mucinous neoplasms of the pancreas J Hepatobiliary Pancreat Surg 13:280-285 doi:10.1007/s00534-005-1056-2

Schmidt D et al. (2012) Waves of retrotransposon expansion remodel genome organization and CTCF binding in multiple mammalian lineages Cell 148:335-348 doi:10.1016/j.cell.2011.11.058

Schoedel KE, Finkelstein SD, Ohori NP (2006) K-Ras and microsatellite marker analysis of fine-needle aspirates from intraductal papillary mucinous neoplasms of the pancreas Diagn Cytopathol 34:605-608 doi:10.1002/dc.20511

Schonleben F et al. (2007) BRAF and KRAS gene mutations in intraductal papillary mucinous neoplasm/carcinoma (IPMN/IPMC) of the pancreas Cancer Lett 249:242-248 doi:10.1016/j.canlet.2006.09.007

Schonleben F, Qiu W, Remotti HE, Hohenberger W, Su GH (2008) PIK3CA, KRAS, and BRAF

mutations in intraductal papillary mucinous neoplasm/carcinoma (IPMN/C) of the pancreas Langenbecks Arch Surg 393:289-296 doi:10.1007/s00423-008-0285-7

Sessa F et al. (1994) Intraductal papillary-mucinous tumours represent a distinct group of pancreatic neoplasms: an investigation of tumour cell differentiation and K-ras, p53 and c-erbB-2 abnormalities in 26 patients Virchows Archiv : an international journal of pathology 425:357-367

Sohn TA, Yeo CJ, Cameron JL, Hruban RH, Fukushima N, Campbell KA, Lillemoe KD (2004) Intraductal papillary mucinous neoplasms of the pancreas: an updated experience Ann Surg 239:788-797; discussion 797-789

Takeda M et al. (2011) Expansion of CpG methylation in the SFRP2 promoter region during colorectal tumorigenesis Acta Med Okayama 65:169-177

Tanaka M et al. (2012) International consensus guidelines 2012 for the management of IPMN and MCN of the pancreas Pancreatology 12:183-197 doi:10.1016/j.pan.2012.04.004

Wang R, Zhang YW, Chen LB (2010) Aberrant promoter methylation of FBLN-3 gene and clinicopathological significance in non-small cell lung carcinoma Lung cancer 69:239-244 doi:10.1016/j.lungcan.2009.10.009

Wang Z, Yuan X, Jiao N, Zhu H, Zhang Y, Tong J (2012) CDH13 and FLBN3 gene methylation are associated with poor prognosis in colorectal cancer Pathology oncology research : POR 18:263-270 doi:10.1007/s12253-011-9437-0

Wasif N, Bentrem DJ, Farrell JJ, Ko CY, Hines OJ, Reber HA, Tomlinson JS (2010) Invasive intraductal papillary mucinous neoplasm versus sporadic pancreatic adenocarcinoma: a stage-matched comparison of outcomes Cancer 116:3369-3377 doi:10.1002/cncr.25070

Wu J et al. (2011a) Whole-exome sequencing of neoplastic cysts of the pancreas reveals recurrent mutations in components of ubiquitin-dependent pathways Proc Natl Acad Sci U S A 108:21188-21193 doi:10.1073/pnas.1118046108

Wu J et al. (2011b) Recurrent GNAS mutations define an unexpected pathway for pancreatic cyst development Sci Transl Med 3:92ra66 doi:10.1126/scitranslmed.3002543

Yang T et al. (2013) Epigenetic inactivation of EFEMP1 is associated with tumor suppressive function in endometrial carcinoma PLoS One 8:e67458 doi:10.1371/journal.pone.0067458

Yue W et al. (2007) Frequent inactivation of RAMP2, EFEMP1 and Dutt1 in lung cancer by promoter hypermethylation Clinical cancer research : an official journal of the American Association for Cancer Research 13:4336-4344 doi:10.1158/1078-0432.CCR-07-0015

Zhu XJ, Liu J, Xu XY, Zhang CD, Dai DQ (2014) Novel tumor-suppressor gene epidermal growth factor-containing fibulin-like extracellular matrix protein 1 is epigenetically silenced and associated with invasion and metastasis in human gastric cancer Mol Med Rep 9:2283-2292 doi:10.3892/mmr.2014.2135

Figure legends

Figure 1. Bisulfite sequencing of the discrete *EFEMP1* gene promoter regions. (A) Schematic representation of the location of discrete *EFEMP1* gene promoter regions and the result of bisulfite sequencing. The white and gray boxes denote untranslated and translated exon in the *EFEMP1* gene, respectively. The red allow indicates the location of the EMBL_M1 motifs 'TGACATCTGTTGGG', a candidate of CTCF biding site. The black arrow indicates the transcriptional starting site. The blue box indicates the regions of which methylation status was analyzed by Nomoto S et al (2010). The green box indicates the regions of which methylation status was analyzed by Yue W et al (2007) and Sadr-Nabavi et al (2009). Vertical lines indicate CpG sites; white circles represent unmethylated CpGs; and gray circles represent methylated and unmethylated CpGs observed by bisulfite direct sequencing (B) Examples of bisulfite sequencing in region 1 and 2. Each CpG was categorized as unmethylated or methylated CpG. TpG denotes the CpG site consisting of unmethylated CpG only. C/TpG denotes the CpG site consisting of both methylated (CpG) and unmethylated CpGs (TpG).

Figure 2. Methylation analysis of EFEMP1. (A) Results of *EFEMP1* methylation by fluorescent Hi-SA. Blue arrows represent PCR fragments with non-methylation in HhaI sites. Red arrows represent methylated PCR fragments cleaved by HhaI. **(B)** Frequencies of *EFEMP1* methylation according to pathological findings. Kaplan–Meier survival curves for disease-free survival **(C)**, excluding a patient

with remaining cancer at the resected margin, and overall survival **(D)** according to *EFEMP1* promoter methylation status.

Figure 3. Expression analysis of EFEMP1. IHC staining of EFEMP1 in intraductal papillary mucinous neoplasms with strong staining **(A)**, moderate staining **(B)**, and weak staining **(C)**. Association between *EFEMP1* methylation status and IHC staining **(D)**. EFEMP1, epidermal growth factor-containing fibulin-like extracellular matrix protein 1; IHC, immunohistochemical; NA, not available.

Additional Files

Supplementary Figure 1. Kaplan–Meier survival curves for DFS and OS according to clinicopathological characteristics. Kaplan–Meier survival curves for DFS (**A, C,** and **E**) excluding a patient with remaining cancer at the resected margin and OS (**B, D,** and **F**) according to atypical grade, invasive carcinoma by stage I and II, and invasive carcinoma by histological type, respectively. DFS, disease-free survival; NA, not available; OS, overall survival.

Supplementary Figure 2. *KRAS* and *GNAS* mutations in IPMNs. (**A**) and (**B**) demonstrate the mutations occurring in *KRAS* codon 12 and *GNAS* codon 201, respectively. (**C**) Venn diagram of IPMNs with *KRAS* mutations, *GNAS* mutations, and concurrent *KRAS* and *GNAS* mutations. (**D**) Population of IPMNs with mutations in both genes, *KRAS* mutation alone, *GNAS* mutation alone, and wild type of both

genes. Kaplan–Meier survival curves for disease-free survival (**E** and **G**), excluding a patient with remaining cancer at the resected margin, and overall survival (**F** and **H**) according to *KRAS* and *GNAS* mutation status, respectively. IPMN, intraductal papillary mucinous neoplasm; NA, not available.

Table 1. Correlation between characteristics of patients and *EFEMP1* methylation status

			Methylation Status of *EFEMP1* - No (%)									
		All	Unmethylation	Partial methylation	Extensive methylation		Region 1 Unmethylation	Region 1 Methylation		Region 2 Unmethylation	Region 2 Methylation	
		No. (%)	n= 9 (%)	n = 48 (%)	n = 8 (%)	*P* value	n = 55 (%)	n = 10 (%)	*P* value	n = 11 (%)	n = 54 (%)	*P* value
Age, y	Median (range)	68 (39-88)	66 (54-82)	70 (39-81)	71 (51-88)	0.482[a]	63 (39-82)	70 (51-88)	0.716[c]	68 (54-82)	70 (39-88)	0.234[c]
Gender	Female	21 (32)	2 (22)	17 (35)	2 (25)	0.753[b]	19 (35)	2 (20)	0.479[d]	2 (18)	19 (35)	0.48[d]
	Male	44 (68)	7 (78)	31 (65)	6 (75)		36 (76)	8 (80)		9 (82)	35 (65)	
Location	Head, neck and uncinate	34 (52)	6 (67)	24 (50)	4 (50)	0.344[b]	29 (53)	5 (50)	1[a]	7 (64)	27 (50)	0.182[a]
	Body and tail	29 (45)	2 (22)	23 (48)	4 (50)		24 (44)	5 (50)		3 (27)	26 (48)	
	Whole pancreas	2 (3)	1 (11)	1 (2)	0 (0)		2 (4)	0 (0)		1 (9)	1 (2)	
Duct involvement*	MD-IPMN	21 (33)	4 (44)	14 (30)	3 (38)	0.896[b]	16 (30)	5 (50)	0.473[d]	6 (55)	15 (28)	0.261[a]
	BD-IPMN	20 (31)	3 (33)	15 (32)	2 (25)		18 (33)	2 (20)		3 (27)	17 (32)	
	Mixed type	23 (36)	2 (22)	18 (38)	3 (38		20 (37)	3 (30)		2 (18)	21 (40)	
Cystic size**, cm	Median size (range)	2.7 (0.5-7.5)	2.6 (0.5-6.7)	2.7 (0.5-7.5)	3.9 (0.5-6.1)	0.872[a]	2.7 (0.5-7.5)	2.7 (0.5-6.1)	0.958[c]	1.7 (0.5-6.7)	2.9 (0.5-7.5)	0.517[c]
	< 3.0cm	35 (54)	5 (56)	27 (56)	3 (38)	0.657[b]	30 (55)	5 (50)	1[d]	7 (64)	28 (52)	0.526[d]
	> 3.0cm	30 (46)	4 (44)	21 (44)	5 (63)		25 (46)	5 (50)		4 (36)	26 (48)	
Main duct diameter, cm	Median size (range)	0.7 (0.2-7.1)	0.6 (0.2-6.7)	0.7 (0.2-7.1)	0.6 (0.2-4.0)	0.822[a]	2.7 (0.5-7.5)	2.7 (0.5-6.2)	0.82[a]	0.7 (0.2-6.7)	0.7 (0.2-7.1)	0.441[a]
	< 1.0cm	45 (69)	6 (67)	33 (69)	6 (75)	1[b]	39 (71)	6 (60)	0.482[b]	6 (54)	39 (72)	0.292[b]
	> 1.0cm	20 (31)	3 (33)	15 (31)	2 (25)		16 (29)	4 (40)		5 (46)	15 (28)	
Presence of mural nodule	Yes	38 (59)	5 (56)	25 (52)	8 (100)	**0.032[a]**	29 (53)	9 (90)	**0.037[a]**	6 (55)	32 (59)	1[a]
	No	27 (42)	4 (44)	23 (48)	0 (0)		26 (47)	1 (10)		5 (46)	22 (41)	
Histologic subtype	Gastric	33 (51)	6 (67)	25 (52)	2 (25)	**0.027[a]**	31 (56)	2 (20)	**0.006[a]**	6 (55)	27 (50)	0.756[a]
	Intestinal	25 (39)	3 (33)	20 (42)	2 (25)		21 (38)	4 (40)		5 (46)	20 (37)	
	Pancreatobillary	6 (9)	0 (0)	2 (4)	4 (50)		2 (4)	4 (40)		0 (0)	6 (11)	
	Oncocytic	1 (2)	0 (0)	1 (2)	0 (0)		1 (2)	0 (0)		0 (0)	1 (2)	
Atypical grade	Low grade	31 (48)	5 (56)	26 (54)	0 (0)	**0.0016[a]**	30 (55)	1 (10)	**0.00044[a]**	6 (55)	25 (46)	0.908[a]
	High grade	11 (17)	1 (11)	11 (21)	0 (0)		11 (20)	0 (0)		1 (9)	10 (19)	
	Invasive Ca	23 (35)	3 (33)	12 (25)	8 (100)		14 (26)	9 (90)		4 (36)	19 (35)	
KRAS	Mutant	33 (51)	3 (33)	25 (52)	5 (63)	0.471[b]	26 (47)	7 (70)	0.303[d]	5 (46)	28 (52)	0.751[a]
	Wild type	32 (49)	6 (67)	23 (48)	3 (38)		29 (53)	3 (30)		6 (55)	26 (48)	
GNAS	Mutant	19 (29)	4 (44)	15 (31)	0 (0)	0.102[a]	19 (35)	0 (0)	**0.028[a]**	4 (36)	15 (28)	0.718[a]
	Wild type	46 (71)	5 (56)	33 (69)	8 (100)		36 (66)	10 (100)		7 (64)	39 (72)	
Combined mutational type	Mutant in the both genes	11 (17)	2 (22)	9 (19)	0 (0)	0.364[b]	11 (20)	0 (0)	0.058[d]	2 (18)	9 (17)	0.899[d]
	KRAS mutation alone	22 (34)	1 (11)	16 (33)	5 (63)		15 (27)	7 (70)		3 (27)	19 (35)	
	GNAS mutation alone	8 (12)	2 (22)	6 (13)	0 (0)		8 (15)	0 (0)		2 (18)	6 (11)	
	Wild type in the both genes	24 (37)	4 (44)	17 (35)	3 (38)		21 (38)	3 (30)		4 (36)	20 (37)	

* One unknown case was excluded

**Cystic size reprsented the largest one measured by CT or MRI

a. *P* value were calculated among unmethylation, partial methylation and extensive methylation by Kruskal-Wallis test

b. *P* value were calculated among unmethylation, partial methylation and extensive methylation by Fisher exact test

c. *P* value were calculated between unmethylation and methylation of region 1 or 2 within *EFEMP1* promoter by Mann-Whitney U test

d. *P* value were calculated between unmethylation and methylation of region 1 or 2 within *EFEMP1* promoter by Fisher exact test

Low grade, Low grade dysplasia ; high grade, high grade dysplasia; invasive Ca, invasive carcinoma; MD-IPMN, main duct type IPMN; BD-IPMN, branch duct type IPMN

Table 2. Methylation status of EFEMP1and Genetic profiles of KRAS and GNAS in this cohort

Sample No.	Gender	Age	Duct involvement	*KRAS*	*GNAS*	*EFEMP* Region 1	*EFEMP* Region 2
Low grade							
14	M	71	MD	WT	WT	U	U
44	M	54	Mixed	WT	WT	U	U
47	M	58	MD	WT	WT	U	U
46	M	63	BD	WT	R201C	U	U
7	F	66	BD	WT	WT	U	U
22	F	63	Mixed	WT	WT	U	M
50	M	68	Mixed	WT	WT	U	M
54	F	76	BD	WT	WT	U	M
60	M	66	Mixed	WT	WT	U	M
65	M	63	MD	WT	WT	U	M
39	M	64	BD	WT	R201C	U	M
42	M	59	MD	G12V	WT	M	U
56	M	65	BD	G12V	R201C	U	M
17	F	71	BD	WT	WT	U	M
21	M	67	BD	WT	WT	U	M
31	M	78	MD	WT	WT	U	M
35	F	57	BD	WT	WT	U	M
36	F	62	BD	WT	WT	U	M
2	M	61	Mixed	WT	WT	U	M
58	M	60	BD	WT	R201H	U	M
13	F	74	MD	G12R	WT	U	M
30	M	73	Mixed	G12D	WT	U	M
57	M	74	Mixed	G12R	WT	U	M
67	M	81	BD	G12D	WT	U	M
55	F	71	MD	G12V	R201C	U	M
41	M	50	BD	G12D	WT	U	M
1	F	65	Mixed	G12V	R201H	U	M
69	M	71	Mixed	G12D	R201S	U	M
18	M	68	BD	WT	R201C	U	M
25	M	69	Mixed	G12D	R201C	U	M
9	M	73	Mixed	G12V	R201C	U	M
High grade							
12	M	81	MD	WT	WT	U	M
16	M	72	MD	WT	WT	U	M
33	F	70	Mixed	G12D	WT	U	M
43	M	75	Mixed	G12V	R201H	U	M
66	M	79	Mixed	WT	R201C	U	M
19	F	67	Mixed	G12R	WT	U	M
38	M	66	Mixed	G12D	R201H	U	U
8	M	73	Mixed	WT	WT	U	M
3	M	70	MD	G12V	WT	U	M
34	F	59	BD	WT	WT	U	M
53	M	72	MD	WT	R201C	U	M
Invasive Ca							
48	66	F	Mixed	WT	WT	U	M
49	67	M	MD	WT	R201C	U	U
10	73	M	MD	G12V	WT	M	U
37	59	F	Unknown	G12V	WT	U	M
4	73	F	MD	G12V	WT	U	M
59	66	M	Mixed	G12V	WT	U	U
6	82	F	MD	G12D	R201C	U	U
20	M	74	MD	G12D	R201H	U	M
32	56	M	BD	WT	WT	U	M
11	74	M	MD	WT	R201C	U	M
52	51	M	Mixed	G12R	WT	M	M
68	78	M	MD	WT	WT	M	M
15	67	M	MD	G12D	WT	M	M
24	72	F	BD	G12V	WT	U	M
51	57	M	MD	G12D	WT	U	M
62	81	F	BD	G12V	R201C	U	M
63	75	M	BD	WT	WT	M	M
70	57	M	Mixed	WT	WT	M	M
5	74	F	MD	G12V	WT	U	M
40	39	M	Mixed	G12V	WT	M	M
64	63	M	BD	G12D	WT	M	M
26	79	F	MD	G12V	WT	M	M
61	88	M	Mixed	G12R	WT	M	M

M, methylation; U, unmethylation; MD, MD-IPMN; BD, BD-IPMN; Mixed, Mixed-IPMN.

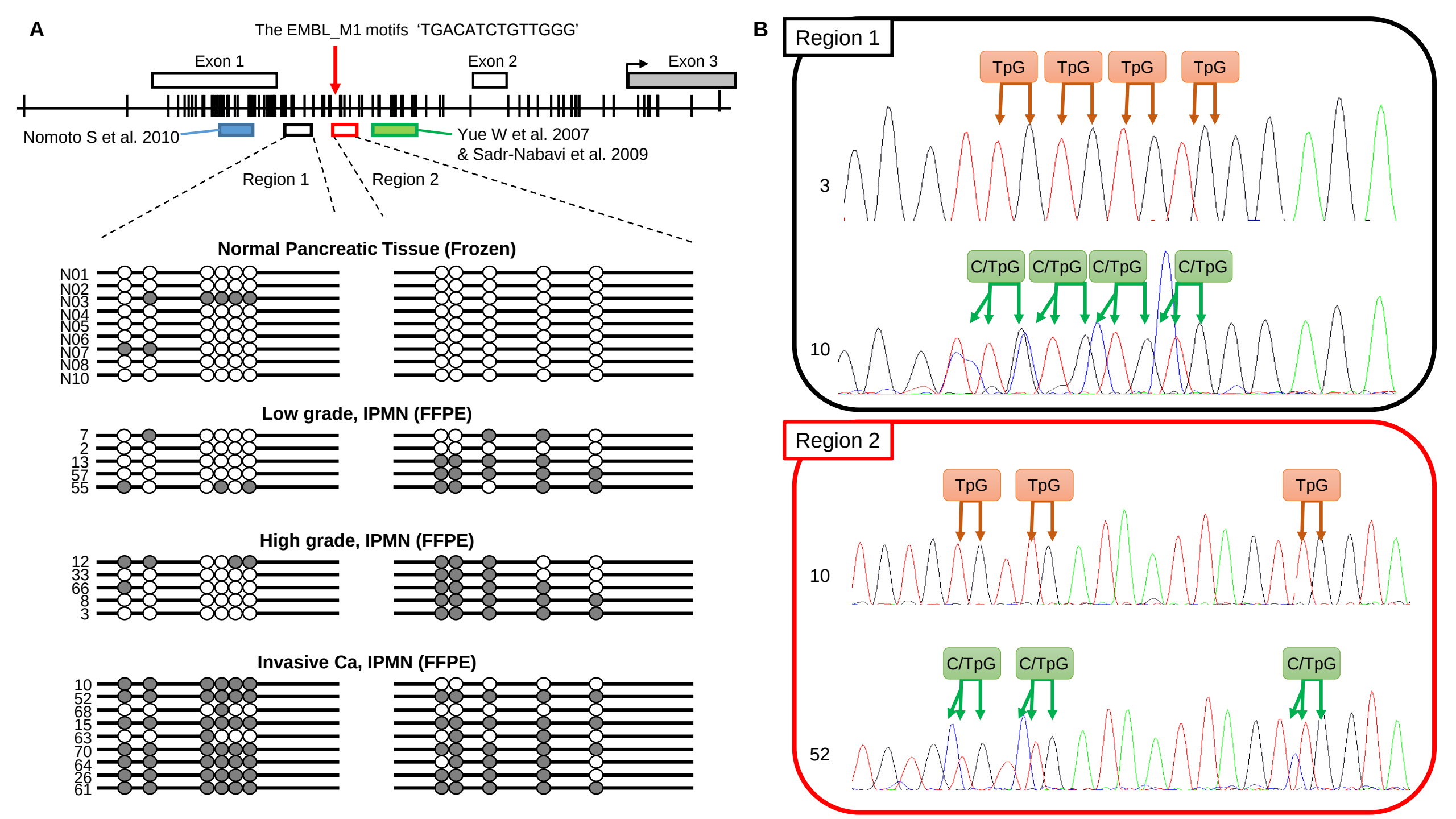
A
The EMBL_M1 motifs 'TGACATCTGTTGGG'
Exon 1
Exon 2
Exon 3
Nomoto S et al. 2010
Yue W et al. 2007
& Sadr-Nabavi et al. 2009
Region 1
Region 2
Normal Pancreatic Tissue (Frozen)
N01
N02
N03
N04
N05
N06
N07
N08
N10
Low grade, IPMN (FFPE)
7
2
13
57
55
High grade, IPMN (FFPE)
12
33
66
8
3
Invasive Ca, IPMN (FFPE)
10
52
68
15
63
70
64
26
61
B
Region 1
TpG
TpG
TpG
TpG
3
C/TpG
C/TpG
C/TpG
C/TpG
10
Region 2
TpG
TpG
TpG
10
C/TpG
C/TpG
C/TpG
52

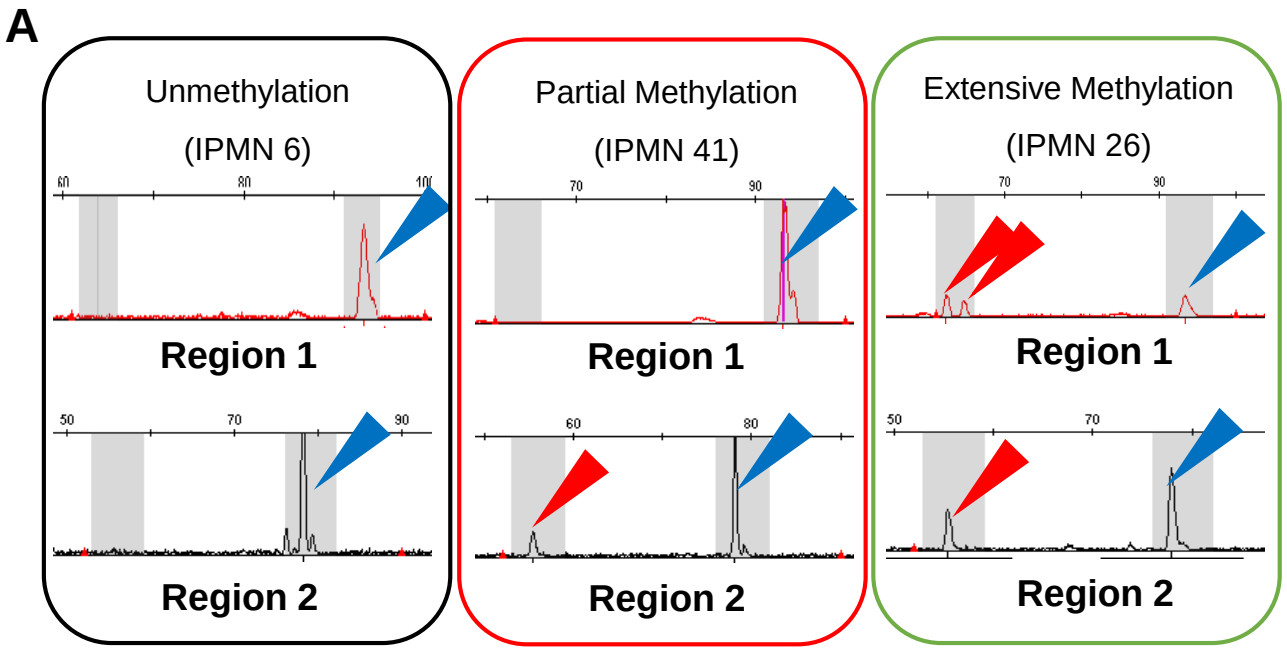

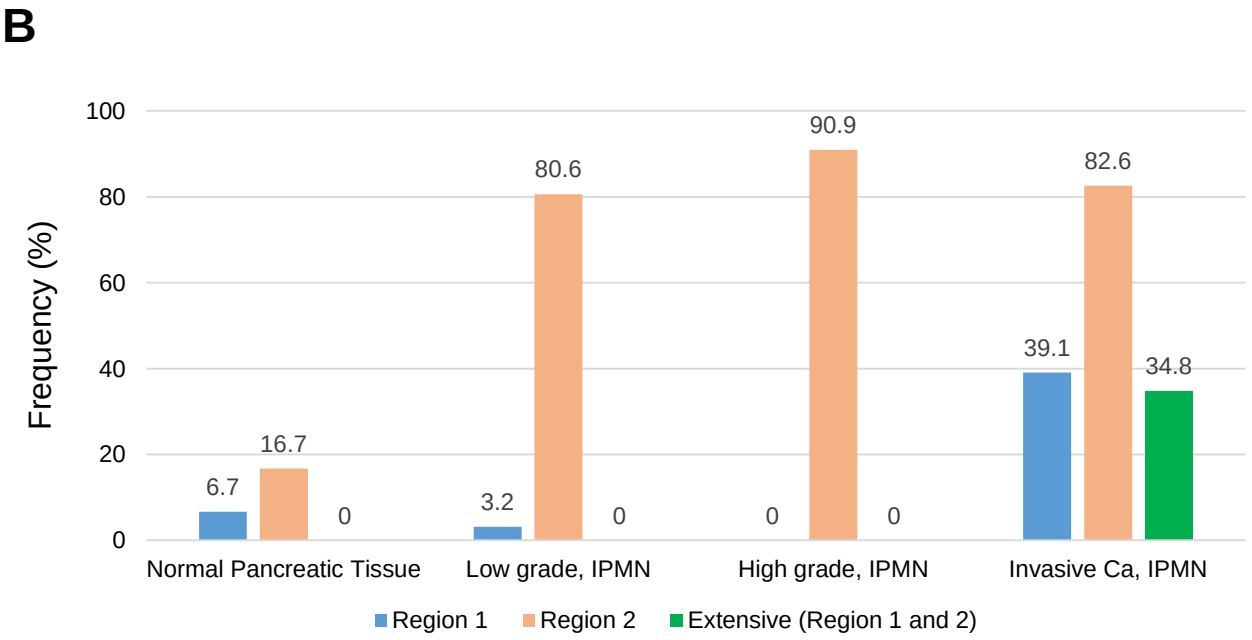

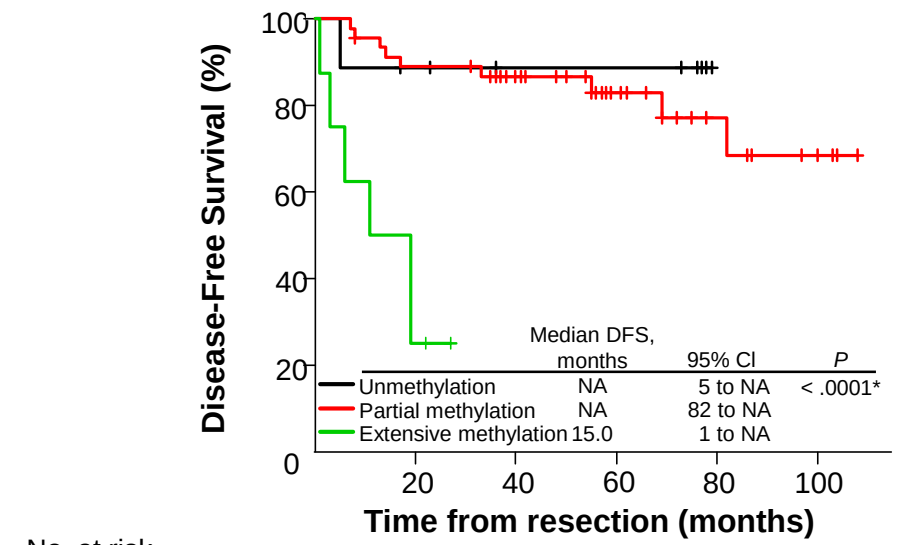

No. at risk

Unmethylation	9	7	5	5	0	0
Partial methylation	46	40	32	17	9	5
Extensive methylation	8	2	0	0	0	0

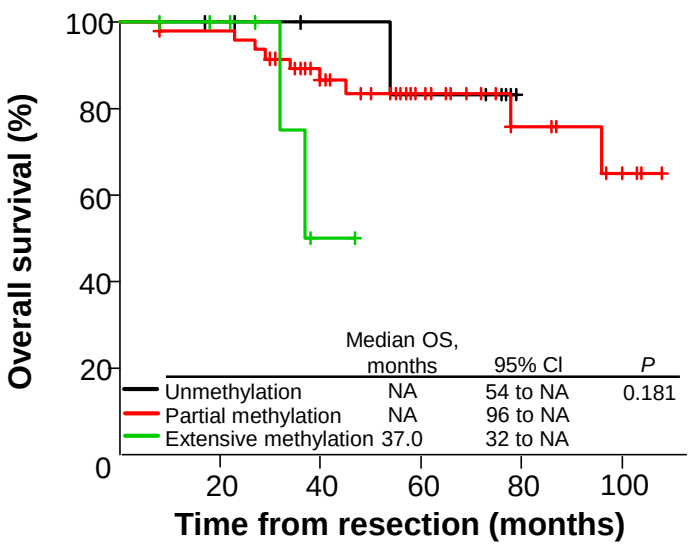

No. at risk

Unmethylation	9	8	6	5	0	0
Partial methylation	48	46	34	18	9	5
Extensive methylation	8	6	1	0	0	0

A

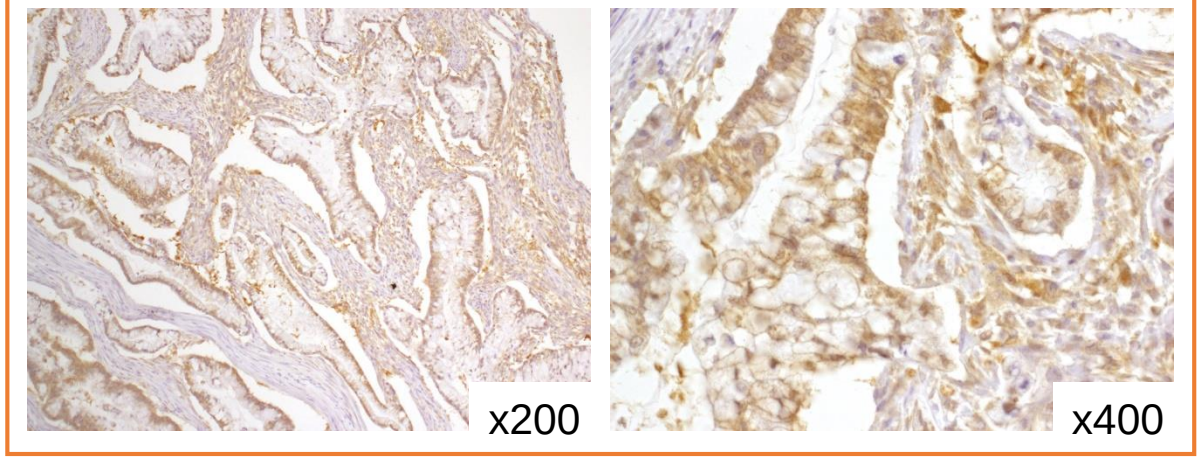
x200
x400

B

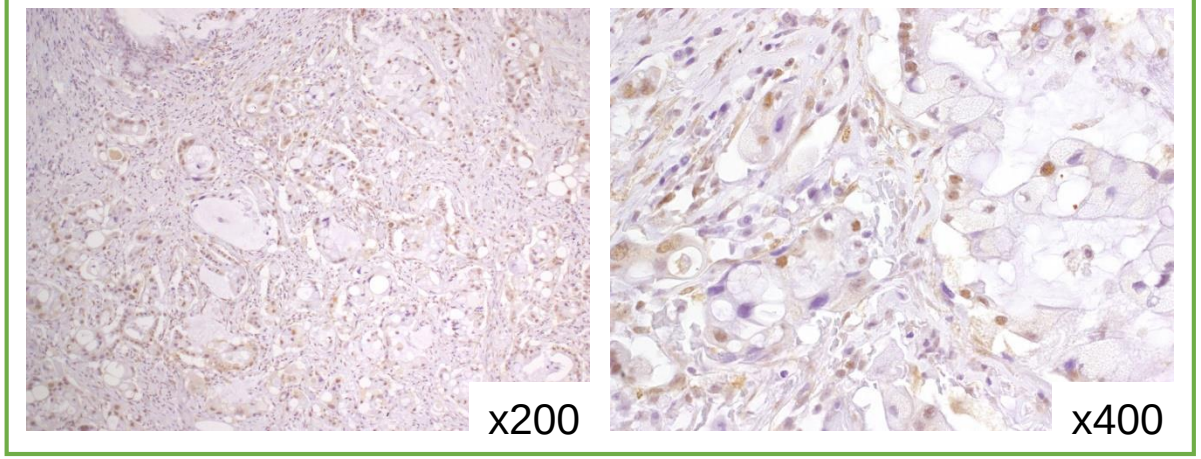
x200
x400

C

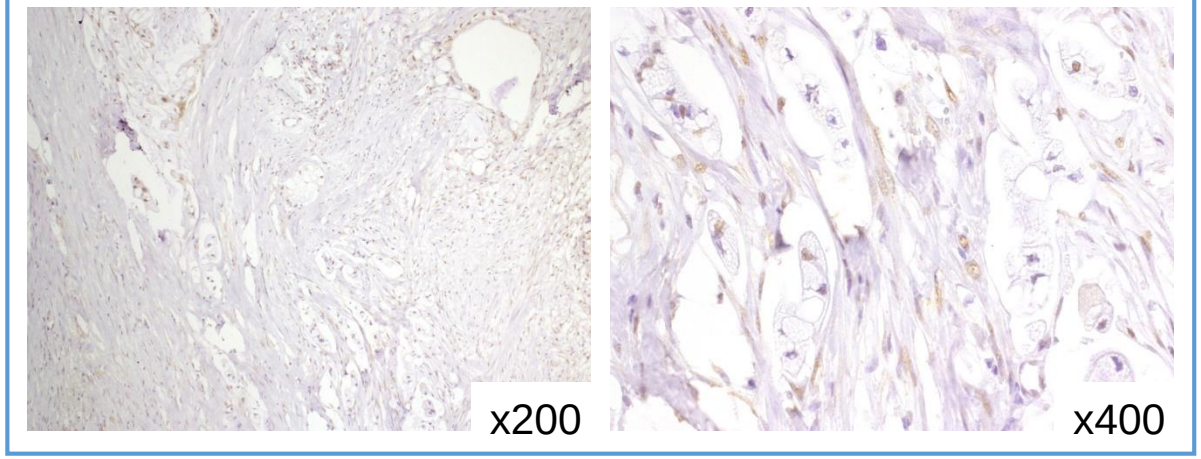
x200
x400

D

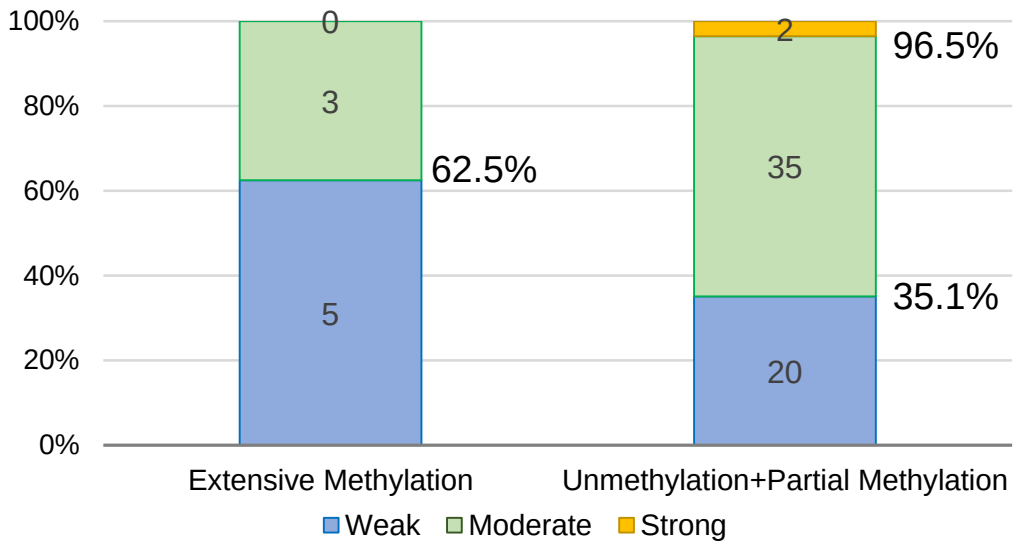
100%
80%
60%
40%
20%
0%
0
3
5
2
35
20
62.5%
96.5%
35.1%
Extensive Methylation
Unmethylation+Partial Methylation
Weak
Moderate
Strong

Supplementary Table 1. Characteristics of IPMN patients

		All	Low grade	High grade	Invasive Ca	*P* value
		No. (%)	n = 31 (%)	n = 11 (%)	n = 23 (%)	
Age, y	Median (range)	68 (39-88)	66 (50-81)	72 (59-81)	72 (39-88)	0.087[a]
Gender	Female	21 (32)	9 (29)	3 (27)	9 (39)	0.608[b]
	Male	44 (68)	22 (71)	8 (73)	14 (61)	
Location	Head, neck and uncinate	34 (52)	17 (55)	6 (55)	11 (48)	0.598[b]
	Body and tail	29 (44)	14 (45)	5 (46)	10 (44)	
	Whole pancreas	2 (3)	0 (0)	0 (0)	2 (9)	
Duct involvement*	MD-IPMN	21 (33)	6 (19)	4 (36)	11 (50)	**0.033[b]**
	BD-IPMN	20 (31)	14 (45)	1 (9.1)	5 (23)	
	Mixed type	23 (36)	11 (36)	6 (55)	6 (27)	
Cystic size**, cm	Median size (range)	2.7 (0.5-7.5)	2.8 (0.5-7.5)	3.2 (0.7-5.0)	1.8 (0.5-7.5)	0.880[a]
	< 3.0cm	35 (54)	17 (53)	8 (67)	15 (65)	1[b]
	> 3.0cm	30 (46)	14 (47)	4 (33)	8 (35)	
Main duct diameter, cm	Median size (range)	0.7 (0.2-7.1)	0.5 (0.2-6.0)	0.7 (0.3-4.7)	0.7 (0.2-7.1)	**0.040[a]**
	< 1.0cm	45 (69)	24 (77)	7 (67)	14 (60)	0.191[b]
	> 1.0cm	20 (31)	7 (23)	4 (33)	9 (40)	
Presence of mural nodule	Yes	38 (59)	13 (58)	9 (81)	16 (70)	**0.013[b]**
	No	27 (42)	18 (42)	2 (18)	7 (30)	
Histologic subtype	Gastric	33 (51)	19 (61)	5 (46)	9 (39)	0.178[b]
	Intestinal	25 (39)	11 (36)	5 (46)	9 (39)	
	Pancreatobillary	6 (9)	1 (3)	0 (0)	5 (22)	
	Oncocytic	1 (2)	0 (0)	1 (9)	0 (0)	
KRAS	Mutant	33 (51)	12 (39)	6 (55)	16 (70)	0.084[b]
	Wild type	32 (49)	19 (61)	5 (46)	7 (30)	
GNAS	Mutant	19 (29)	10 (32)	7 (64)	5 (22)	0.785[b]
	Wild type	46 (71)	21 (68)	4 (36)	18 (78)	
Combined mutational type	Mutant in the both genes	11 (17)	6 (19)	2 (18)	3 (13)	0.110[b]
	KRAS mutation alone	22 (34)	6 (19)	3 (27)	13 (57)	
	GNAS mutation alone	8 (12)	4 (13)	2 (18)	2 (9)	
	Wild type in the both genes	24 (37)	15 (48)	4 (36)	5 (22)	

* One unknown case was excluded

**Cystic size reprsented the largest one measured by CT or MRI

a. *P* values were calculated between Low-grade and High-grade/Invasive Ca by Mann-Whitney U test

b. *P* values were calculated between Low-grade and High-grade/Invasive Ca by Fisher exact test

Low grade, Low grade dysplasia ; high grade, high grade dysplasia; invasive Ca, invasive carcinoma; MD-IPMN, main duct type IPMN; BD-IPMN, branch duct type IPMN

Supplementary Table 2. Characteristics of patients with invasive Ca

Characteristic		n (%)
TNM Stage	IA/IB	10 (44)
	IIA/IIB	12 (52)
	III	0 (0)
	IV	1 (4)
Tumor stage	T1 and T2	13 (57)
	T3 and T4	10 (44)
Nodal metastasis	Negative	17 (74)
	Positive	6 (26)
Distant metastasis	Negative	22 (96)
	Positive	1 (4)
Histology	Tubular carcinoma	13 (57)
	Colloid carcinoma	8 (35)
	Papillary/Poor differentiation	2 (9)

Supplementary Table 3. Primer sequence

GNAS		Forward	5’-GATTGGCAATTATTACTGTTTC-3’
		Reverse	5’-GGAGGAGGCAGCTGGTTATTC-3’
EFEMP1-HiSA	Region-1		
		Forward	5'-TTYGAGYGAGTTTAGTATTTATTGGGT-3'
		Reverse	5'-CTACACAATCCAAAACAATTCTC-3'
	Internal Methylation	Specific	5'-TTCGAGCGAGTTTAGTATTTATTGGGTC-3'
	Region-2		
		Forward	5'-TTGTTGGGATGGGTATGTGTGT-3'
		Reverse	5'-TAATCCCCTAAACTTTCAAAACCA-3'
	Internal Methylation	Specific	5'-TTGTTGGGATGGGTATGTGTGTGC-3'
EFEMP1-Direct Sequence	Region-1		
		Forward	5'-GGTCGTATAGGTAGGAGTTTTTAA-3'
		Reverse	5'-CCTACACAATCCAAAACAATTCTC-3'
	Region-2		
		Forward	5'-GAGTATTCGGGTGATATTTGTTG-3'
		Reverse	5'-AACCAACTCCTATAAAATCCAAAT-3'

A

KRAS Codon 12

GGT to G*T*T (G12V)

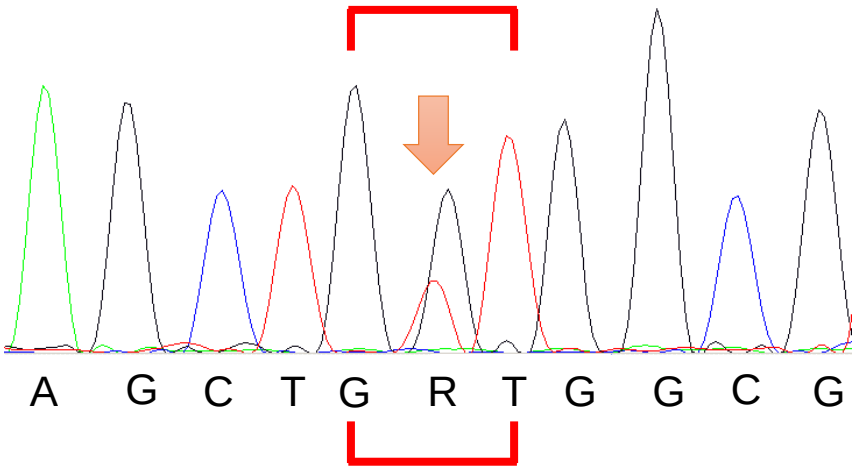

B

GNAS Codon 201

CGT to *T*GT (R201C)

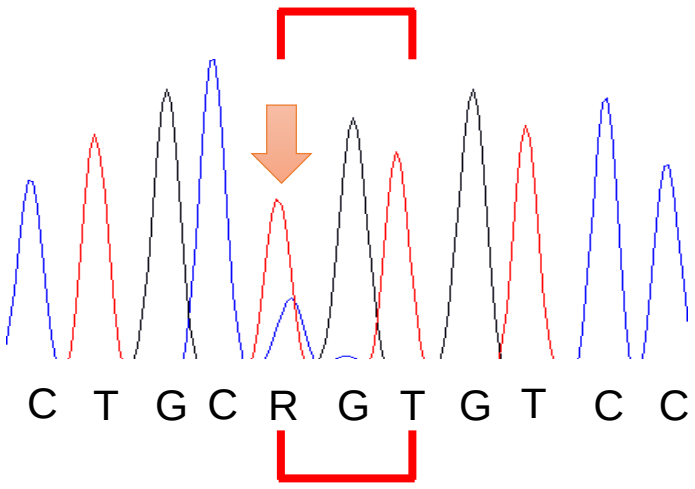

C

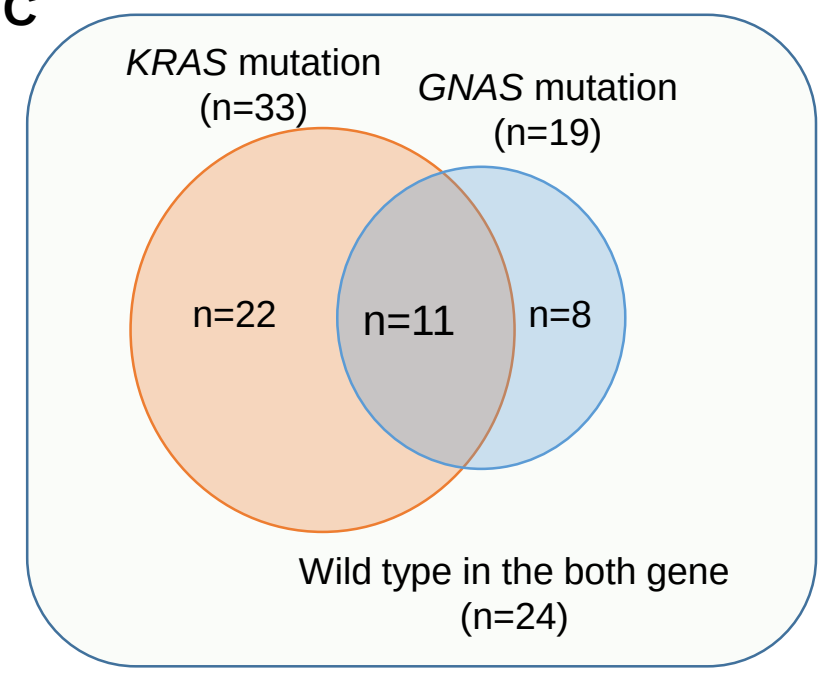

D

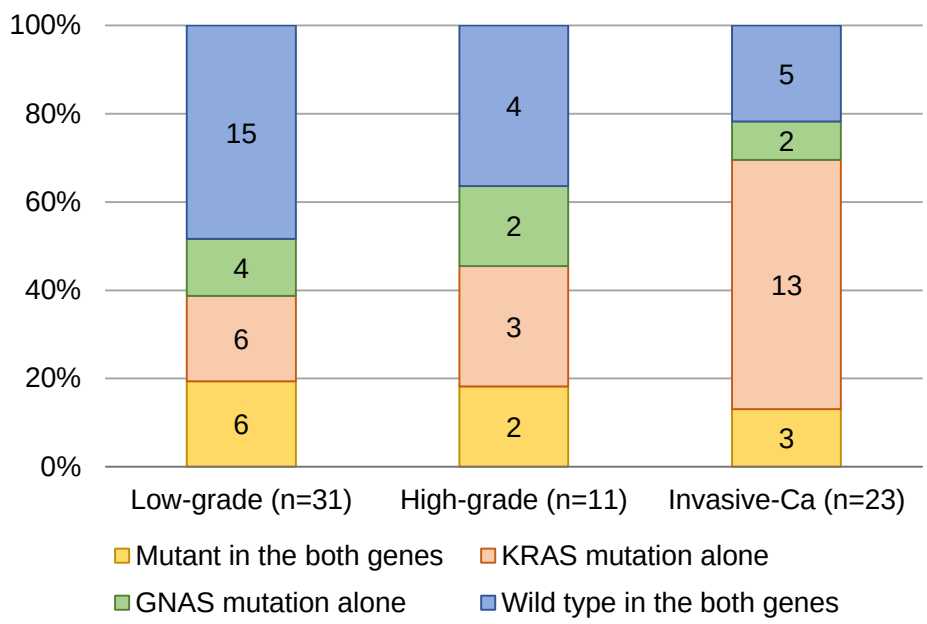

E

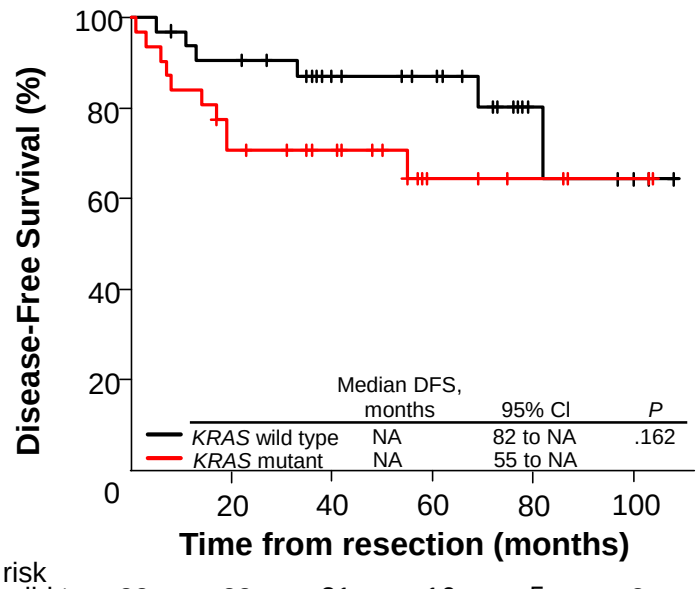

No. at risk						
KRAS wild type	32	28	21	16	5	3
KRAS mutant	31	21	16	6	4	2

F

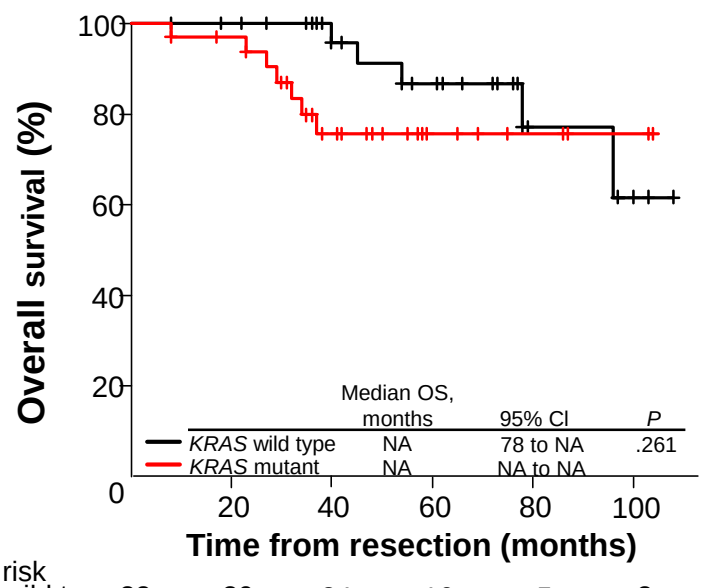

No. at risk						
KRAS wild type	32	30	24	16	5	3
KRAS mutant	33	30	17	7	4	2

G

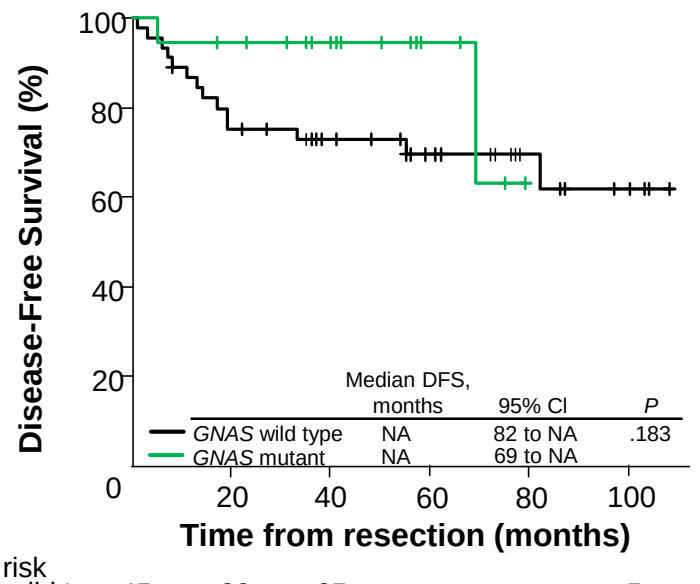

No. at risk						
GNAS wild type	45	33	25	18	9	5
GNAS mutant	18	16	12	4	0	0

H

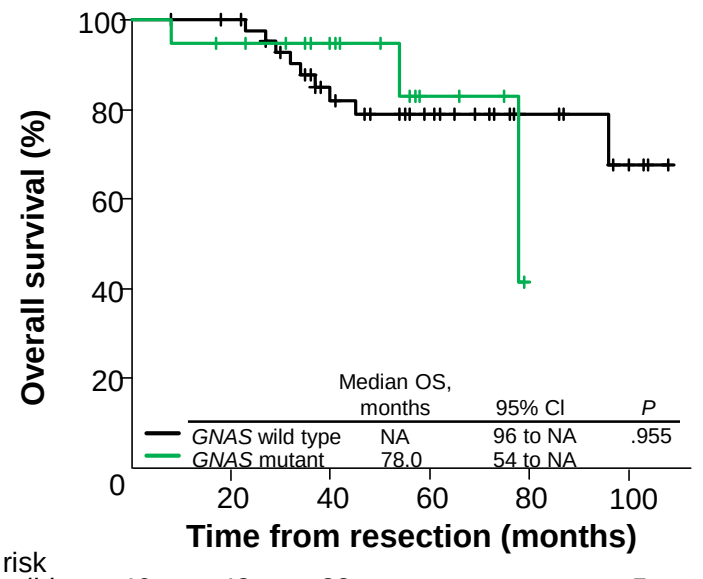

No. at risk						
GNAS wild type	46	43	28	19	9	5
GNAS mutant	19	17	13	4	0	0